

Thick Strip Model for Numerical Investigations on VIV of a Flexible Cylinder

Di Deng, Lei Wu, Decheng Wan*

State Key Laboratory of Ocean Engineering, School of Naval Architecture, Ocean and Civil Engineering, Shanghai Jiao Tong University, Collaborative Innovation Center for Advanced Ship and Deep-Sea Exploration, Shanghai 200240, China

*Corresponding author: dcwan@sjtu.edu.cn

Abstract

With the increase of oil exploitation, the aspect ratio of marine risers increases so apparently that leads to the prediction on VIV response becoming more difficult and the computational domain becoming larger. In this paper, numerical simulations on VIV of a flexible cylinder experiencing uniform and stepped flow adopting the thick strip method are conducted through the in-house viv-FOAM-SJTU solver. Hydrodynamic forces are calculated in each thick fluid strip distributed equidistantly along the cylinder. The connection among all thick strips is realized through the calculation of the structural vibration in both in-line and cross-flow directions, using the finite element method (FEM) with the Euler-Bernoulli beam model. Comparisons between experimental results and present studies show good agreement, which represents the feasibility of the thick strip method in solving VIV response of flexible cylinder. Meanwhile, the apparent three-dimensional effect is captured. It can also be found that vortex shedding features vary at each thick strip along different locations of the cylinder.

Keywords: vortex-induced vibration; thick strip method; flexible cylinder

1. Introduction

Alternant vortex shedding phenomenon will happen when viscous flow goes through the circular cylinder, which contributes to the vortex-induced vibration problem especially for the offshore structures and risers. VIV of flexible cylinders has been extensively studied during the past decades. Overviews on VIV researches can be referred to Sarpkaya (2004), Huang et al (2009), Chen et al (2016) and Wan et al (2017). In order to solve the problems of high costs of computational resources and long computing time, the traditional strip method, which considered that the fluid flow was locally two-dimensional without spanwise correlation and simplified the three-dimensional fluid field into several two-dimensional strips, was proposed and used to predict the VIV response of risers by Willden and Graham (2001, 2004). Adopting the strip method, Duan et al (2016, 2018) developed the viv-FOAM-SJTU solver and carried out numerical simulations on VIV of a vertical riser exposed to the stepped current basing on the experiments of Chaplin et al (2005). Fu et al (2016) conducted parameter researches on VIV of a flexible cylinder using the viv-FOAM-SJTU solver. Fu et al (2018) then further expanded the capacity to simulations of a flexible cylinder experiencing oscillatory flow and validate its reliability with standard model experiments of Fu et al (2013).

In order to solve the drawback in simulating the axial three-dimensional correlation of vortex shedding, the three-dimensional simulation method was adopted and used by researchers in predicting VIV response. Holmes et al (2006) combined three-dimensional CFD solutions

with structural models in simulating VIV of a straked riser. Huang et al (2007a, 2007b) presented a CFD approach for riser VIV prediction using the URANS method on an three-dimensional overset grid system. Numerical results on VIV of a flexible riser experiencing uniform flow and sheared flow were in good agreement with experimental results and previous publications. Wang and Xiao (2016) adopted the large eddy simulation (LES) method with the Arbitrary Lagrangian-Eulerian (ALE) scheme in simulating VIV response of a riser in uniform flow and sheared flow respectively using the ANSYS MFX multi-field solver.

Although the three-dimensional numerical simulation method can cover disadvantages in simulating flow fields comparing with the traditional strip method, the cost of computational resources are extremely larger especially for detailed flow fields simulation. Combining advantages of the axial correlation for the three-dimensional method and the low computational resource cost for the traditional strip method, Bao et al (2016) proposed the thick strip model for VIV prediction of long flexible cylinder using the direct numerical simulation (DNS) method. Comparisons between experimental results and simulation results validate the validity of the thick strip method.

In this paper, the modified viv-FOAM-SJTU solver is used to predict VIV response of a flexible cylinder exposed to uniform flow and stepped flow respectively basing on the thick strip method. This paper is organized as follows: The first section gives a brief introduction to the referenced experiments and the numerical methodology. The second section presents the results and the final section concludes the paper.

2. Method

2.1 Thick Strip Method

The schematic of the strip theory is shown in Fig.1. The flow field is discreted into several two-dimensional fluid strips equal-distantly located along the span of the cylinder. The strip method owns high computational efficiency and accuracy that has been verified through previous researches, such as Meneghini et al (2004) and Yamamoto et al. (2004). The original viv-FOAM-SJTU solver developed basing on the OpenFOAM and the traditional strip method and detailedly validated by Duan et al (2016). However, the simplification of ignoring the spanwise correlation will lead to the lower prediction of hydrodynamic forces in both inline and crossflow directions. Then, the predicted vibration amplitude will be smaller than that of the experimental results, especially in high Reynolds Number conditions with non-negligible three-dimensional characteristic of vortex shedding along the cylinder span. Bao et al(2016) proposed the generalized thick strip modelling method considering the spanwise correlation in the flow field locally. And this method has been validated in simulating VIV responses of a flexible cylinder experiencing the uniform flow by Bao et al(2019). In this paper, the thick strip model has been used to modify the original viv-FOAM-SJTU solver through transforming the two-dimensional fluid strips into three-dimensional thick fluid strips. While the correlation of fluid strips are realized through the vibration of the cylinder using the Finite Element Method (FEM).

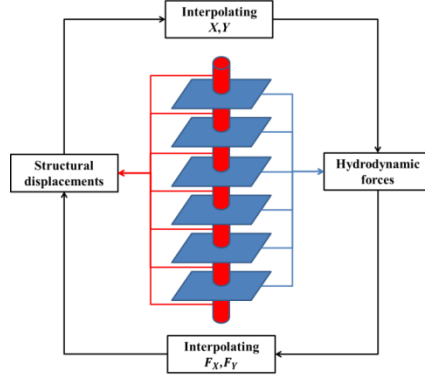


Fig.1 Schematic diagram of the strip theory

2.2 Hydrodynamics Governing Equations

The Reynolds-averaged Navier-Stokes equations (RANS) are used as the hydrodynamics governing equations in all thick flow strips as shown in Eq(1) and Eq(2). The flow field is supposed to be incompressible, with constant dynamic viscosity μ and constant density ρ .

$$\frac{\partial \bar{u}_i}{\partial x_i} = 0 \quad (1)$$

$$\frac{\partial}{\partial t}(\rho \bar{u}_i) + \frac{\partial}{\partial x_j}(\rho \bar{u}_i \bar{u}_j) = -\frac{\partial \bar{p}}{\partial x_i} + \frac{\partial}{\partial x_j}(2\mu \bar{S}_{ij} - \rho \overline{u'_j u'_i}) \quad (2)$$

where $\bar{S}_{ij} = \frac{1}{2} \left(\frac{\partial \bar{u}_i}{\partial x_j} + \frac{\partial \bar{u}_j}{\partial x_i} \right)$ is the mean rate of strain tensor, $-\rho \overline{u'_j u'_i}$ is referred as Reynolds stress τ_{ij} computed through $\tau_{ij} = -\rho \overline{u'_j u'_i} = 2\mu_t \bar{S}_{ij} - \frac{2}{3} \rho k \delta_{ij}$, where μ_t is the turbulent viscosity and $k = (1/2) \overline{u'_i u'_i}$ is the turbulent energy, computing from the fluctuating velocity field.

2.3 Structural Dynamic Governing Equations

Each two-dimensional fluid strip is independent with the connection between all strips realized through the in-line and cross-flow vibration of the cylinder. The flexible cylinder is simplified to be an Euler-Bernoulli bending beam model. The vibration of the model is solved through the FEM method and the structural governing equations in each element are shown in Eq(3) and Eq(4).

$$m\ddot{x} + c\dot{x} + kx = f_x \quad (3)$$

$$m\ddot{y} + c\dot{y} + ky = f_y \quad (4)$$

where m , c , k are the mass, the damping and the stiffness of the structural element; f_x, f_y are the in-line and the cross-flow hydrodynamic forces respectively. Hence, the mass-spring-damping (MCK) equations of the system can be expressed as Eq(5) and Eq(6):

$$\mathbf{M}\{\ddot{\mathbf{X}}\} + \mathbf{C}\{\dot{\mathbf{X}}\} + \mathbf{K}\{\mathbf{X}\} = \{\mathbf{F}_{\text{HX}}\} \quad (5)$$

$$\mathbf{M}\{\ddot{\mathbf{Y}}\} + \mathbf{C}\{\dot{\mathbf{Y}}\} + \mathbf{K}\{\mathbf{Y}\} = \{\mathbf{F}_{\text{HY}}\} \quad (6)$$

where \mathbf{M} , \mathbf{C} , \mathbf{K} are the mass, damping and stiffness matrixes of the system; $\{\mathbf{F}_{\text{HX}}\}, \{\mathbf{F}_{\text{HY}}\}$ are hydrodynamic force vectors in the in-line and cross-flow directions. While, the Rayleigh damping is adopted to generate the damping matrix replacing the practical damping as shown in Eq(7) and Eq(8).

$$\mathbf{C} = a_0 \mathbf{M} + a_1 \mathbf{K} \quad (7)$$

$$\begin{bmatrix} a_0 \\ a_1 \end{bmatrix} = \frac{2\zeta}{f_{n1} + f_{n2}} \begin{bmatrix} 2\pi f_{n1} f_{n2} \\ 1/(2\pi) \end{bmatrix} \quad (8)$$

where a_0 and a_1 are proportionality coefficient; ζ is the damping ratio; f_{n1} and f_{n2} are the first two order of natural frequencies of the cylinder.

2.4 Problem Description

In the present study, two types of flow conditions are mainly considered for VIV of a vertical flexible cylinder, such as uniform flow and stepped flow. For the uniform flow condition, the model experiments were conducted at the MARINTEK by ExxonMobil (Lehn, 2003). Main parameters of the model cylinder and the flow condition are listed in Table 1. Totally, 10 thick strips are equal-distantly located along the cylinder.

For the stepped flow condition, model cylinder experiments are carried by Chaplin et al (2005a, 2005b). Main parameters and the selected flow condition are listed in Table 2. In the stepped flow condition, only the lower 45% part of the cylinder is immersed in the uniform flow with the other part being in the still water. 20 thick strips are adopted to generate the computational model, so that the lower 9 strips set the uniform flow condition and other strips set the still water condition.

Table 1 Main parameters of model cylinder in uniform flow condition

Properties	Values	Unit
L	9.63	m
D	20	mm
EI	135.4	Nm ²
T	817	N
m^*	2.23	-
L/D	481.5	-
U	0.2	m/s

Table 2 Main parameters of model cylinder in stepped flow condition

Properties	Values	Unit
D	0.028	m
L	13.12	m
L/D	469	-
EI	29.88	Nm ²
m^*	3.0	-
T	405	N
U	0.16	m/s

3. Results

3.1 Vibration response

For the uniform flow condition, CFD simulation is conducted using a computational mesh with 7.9 million cells. The maximum crossflow root-mean-square (RMS) response amplitude comparison among experiment (Lehn, 2003), previous simulation of Wang and Xiao (2016) and present simulation is shown in table 3. It can be concluded that both the maximum crossflow RMS amplitude and the corresponding axial location are in good agreement, which validate the validity of the modified viv-FOAM-SJTU solver in predicting VIV response of flexible cylinder. For the stepped flow condition, the maximum crossflow vibration amplitude

is around $0.7D$ in present simulation, while the experimental result is around $0.75D$ and the corresponding computational error is acceptable.

Crossflow spatial RMS amplitude and the corresponding response envelopes in both flow conditions are shown in Fig.2. The crossflow vibration is dominated by the first mode in the uniform flow and the maximum vibration amplitude locates at around the mid-span of the cylinder as shown in Fig.2(a) and Fig.2(b). While the dominant vibration mode presents the second mode for the stepped flow condition in Fig.2(c), which shows good agreement with the experimental results by Chaplin et al (2005). The peak points of the spatial vibration along the cylinder span locate at $0.25L$ and $0.75L$ respectively as shown in Fig.2(d), where L is the total length of the cylinder.

Table 3 Maximum RMS amplitude comparison for the uniform flow condition

	CF RMS	z/L
Lehn (2003)	0.408	0.549
Wang and Xiao (2016)	0.4	0.523
Present simulation	0.417	0.552

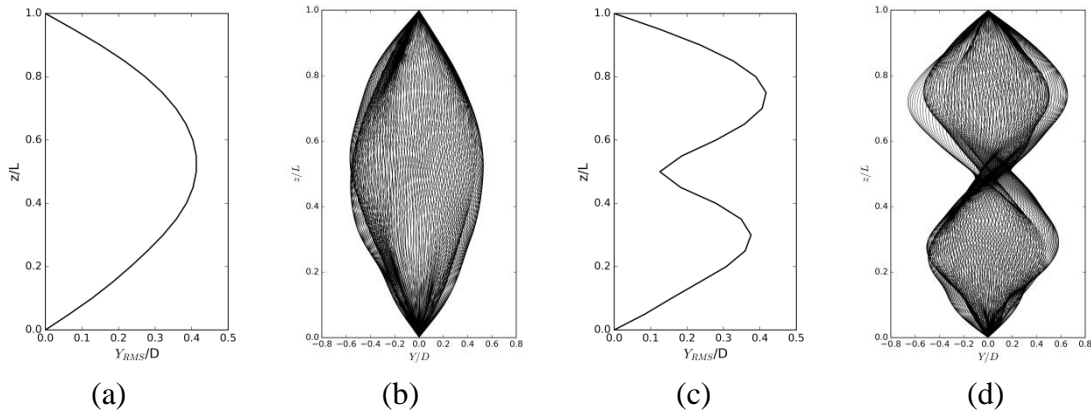


Fig.2 RMS amplitude and response envelopes of the cylinder: (a) uniform flow (b) uniform flow (c) stepped flow (d) stepped flow

Vibration trajectories of specific nodes along the cylinder span are presented in Fig.3. It can be known that the vibration trajectory presents an approximate ‘V’ type at $z/L=0.1$. With the increase of the axial location from the bottom end to the top end, the vibration trajectory turns to be thinner in the inline direction (x direction). The vibration trajectory shape changes to the converse ‘V’ type at $z/L=0.8$.

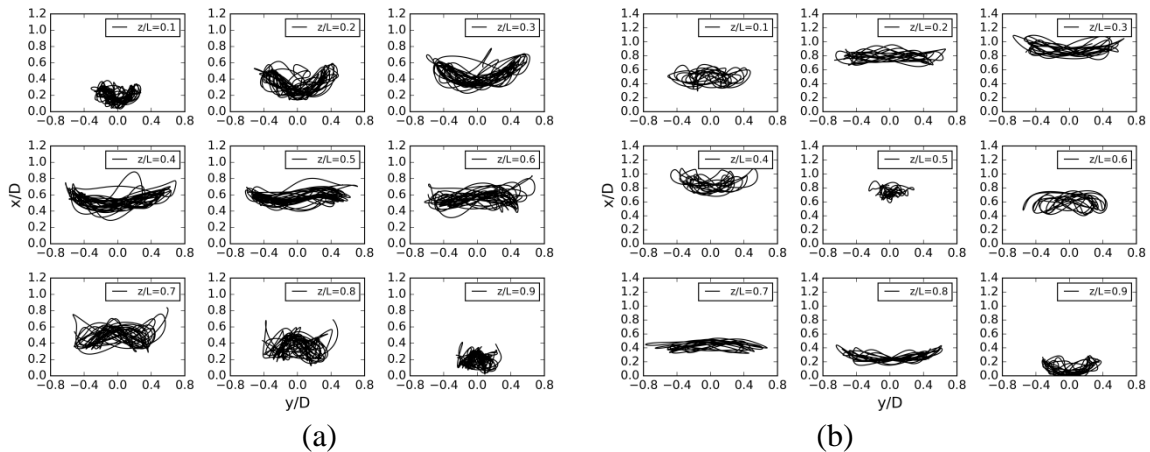


Fig.3 Vibration trajectories along the cylinder span: (a) uniform flow (b) stepped flow

This variation tendency can owe to the interaction between the crossflow vibration and the inline vibration. When the crossflow vibration of lower nodes on the cylinder reaches its maximum value, the corresponding inline vibration amplitude reaches its maximum value at the same time. While, upper nodes on the cylinder present opposite phase between the crossflow vibration and the inline vibration contributing to the converse ‘V’ type of vibration trajectory. As for the middle node on the cylinder, the standing wave point appears that leads to the minimum vibration value and the thinnest trajectory thickness in the inline direction. For the stepped flow condition, the vibration trajectory presents the reverse ‘U’ type at $z/L=0.1, 0.2, 0.6, 0.7$ and the ‘U’ type at $z/L=0.3, 0.4, 0.8, 0.9$. This variation tendency is similar to that of the uniform flow condition owing to the second mode vibration in the crossflow direction and the fourth vibration mode in the inline direction. The maximum inline vibration locates at around $z/L=0.3$. Both the crossflow thickness and the inline thickness of the vibration trajectory turn to the minimum value at the mid span cylinder owing to the existence of standing wave points in both directions.

3.2 Modal response

In order to get the vibration features of the flexible cylinder, the modal decomposition method is adopted, which has been verified to be available by Chaplin et al (2005). The cross-flow and in-line time varying shape of the cylinder can be expressed as the sum of a series of mode shapes as followed:

$$\varphi_n(z) = \sin\left(\frac{n\pi}{L} z\right) \quad (9)$$

$$x(z,t) = \sum_{n=1}^N u_n(t) \cdot \varphi_n(z) \quad (10)$$

$$y(z,t) = \sum_{n=1}^N v_n(t) \cdot \varphi_n(z) \quad (11)$$

where z is the node location along the flexible cylinder span; L is the length of the cylinder; $n=1, 2, 3$, etc; $u_n(t)$ is the time-dependent modal weight in the in-line direction; $v_n(t)$ is the time-dependent modal weight in the cross-flow direction; N is the mode number.

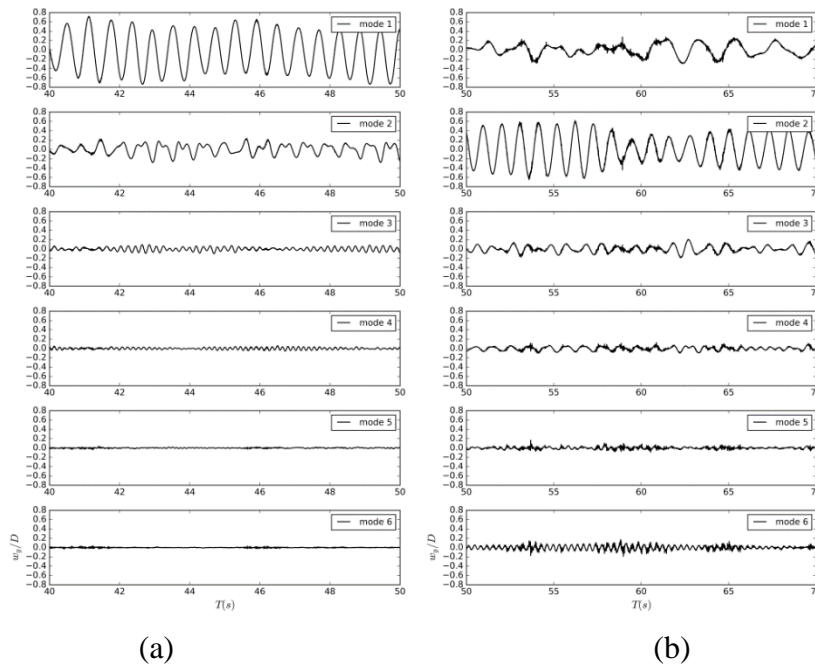


Fig.4 Modal weight of the cylinder vibration: (a) uniform flow (b) stepped flow

Modal weights of the first six order of vibration mode in both flow conditions are shown in Fig.4. It can be known that the dominant vibration mode presents the first mode for the uniform flow condition. Although the second vibration mode is comparatively apparent comparing with other higher modes, it is still unable to transit the vibration of the cylinder to the second mode by the controlling effect of the first mode as shown in Fig.4 (a). As for the stepped flow condition, the dominant vibration mode of the cylinder presents the second mode with effects of other modes on the vibration can be neglected. The mode decomposition results agree well with the experimental results of Lehn(2003) and Chaplin et al(2005) respectively, which also correspond with the response envelopes of the cylinder as shown in Fig.2.

3.3 Frequency response

In order to analyze the frequency feature of the crossflow vibration, the Fast Fourier transform (FFT) method is adopted to calculate the frequency components at specific nodes along the cylinder as shown in Fig.5. From Fig.5 (a), it can be seen that the dominant vibration frequency of nodes along the cylinder is around 1.7Hz in the uniform flow condition. And the vibration response is more conspicuous when close to the mid-span of the cylinder, corresponding to the place where drastic crossflow VIV phenomenon happens. In the stepped flow condition as shown in Fig.5 (b), the dominant vibration frequency is around 0.9Hz. The apparent crossflow VIV phenomenon happens at around $z/L=0.3$ and 0.7 where peak and points appears as shown in Fig.2 (d). The generation of the standing wave point at $z/L=0.5$ leads to the reduction of VIV feature comparing with that of other nodes. The variation of the vibration frequency response along the cylinder is quite similar to that of the amplitude response.

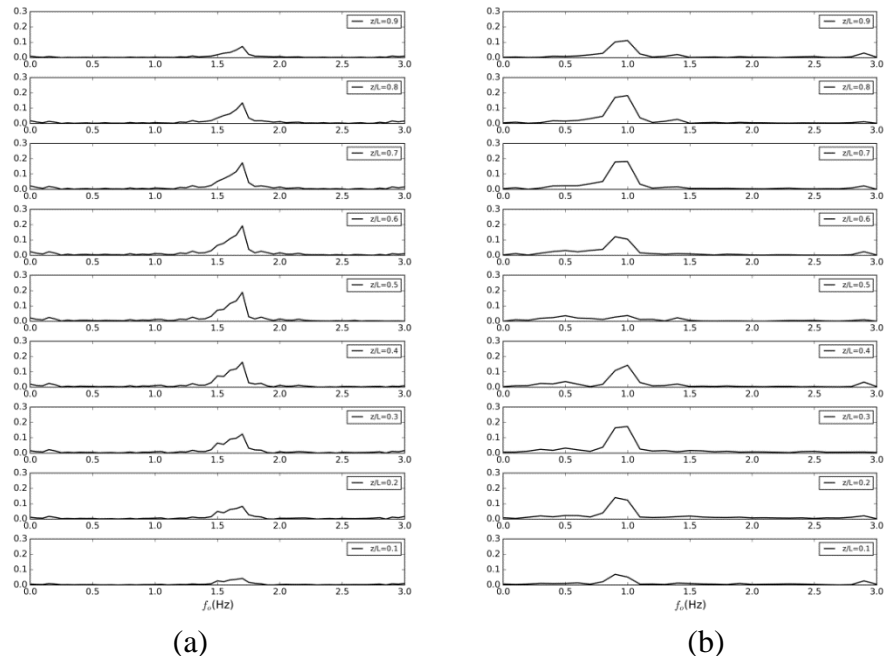


Fig.5 Vibration frequency along the cylinder span: (a) uniform flow (b) stepped flow

3.3 Wake fields

Adopting the flow visualization method, wake flow contours along the cylinder in different flow conditions are shown in Fig.6. On account of the crossflow and the inline vibration, the

wake field turns to be chaotic and shows apparent three-dimensional features. The axial three-dimensional feature becomes more drastic at location close to the mid-span of the cylinder in the uniform flow condition where maximum crossflow vibration amplitude appears. In the stepped flow condition, apparent three-dimensional wake fields appear in the lower 9 strips where vortex shedding direction is the same as the flow speed direction. As for the upper strips that locate in the still water, vortices generate due to the vibration of the cylinder. Apparent vortex shedding phenomenon happens at around $z/L=0.7$ where maximum crossflow vibration amplitude occurs. And the vortex shedding direction is the same as the crossflow vibration direction.

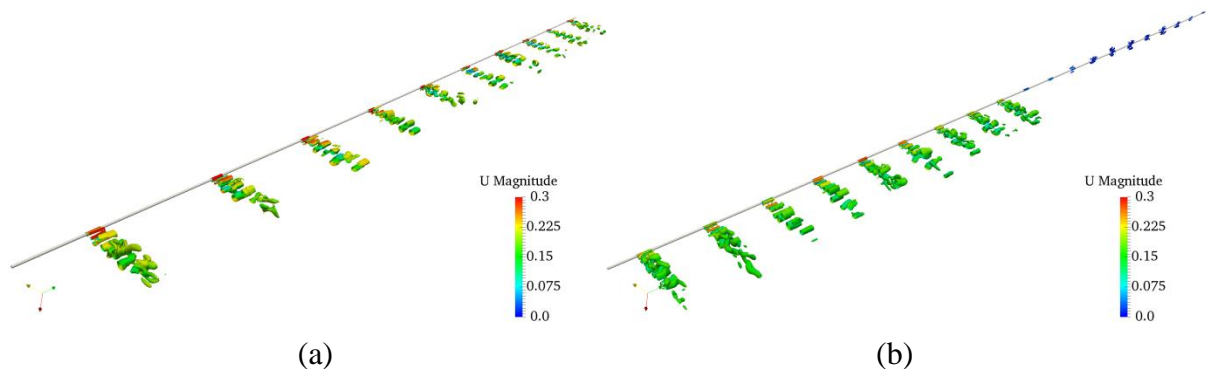


Fig.6 Wake field contour: (a) uniform flow (b) stepped flow

4. Conclusions

In this paper, the thick strip method is adopted to modify the original viv-FOAM-SJTU solver based on the two-dimensional strip method. Two simulations based on model experiments of VIV of a flexible cylinder in uniform flow (Lehn, 2003) and stepped flow (Chaplin, 2005) are conducted using the modified solver. Simulation results are in good agreement with experiment results, which verifies the validity of the thick strip method in predicting VIV response.

Acknowledgements

This work is supported by the National Natural Science Foundation of China (51879159, 51490675, 11432009, 51579145), Chang Jiang Scholars Program (T2014099), Shanghai Excellent Academic Leaders Program (17XD1402300), Program for Professor of Special Appointment (Eastern Scholar) at Shanghai Institutions of Higher Learning (2013022), Innovative Special Project of Numerical Tank of Ministry of Industry and Information Technology of China (2016-23/09) and Lloyd's Register Foundation for doctoral student, to which the authors are most grateful.

Reference

- [1] Bao Y., Palacios R., Graham M., et al. Generalized thick strip modelling for vortex-induced vibration of long flexible cylinders[J]. *Journal of Computational Physics*, 2016, 321(800), 1079–1097.
- [2] Bao Y., Zhu H.B., Huan P., et al. Numerical prediction of vortex-induced vibration of flexible riser with thick strip method[J]. *Journal of Fluids and Structures*, 2019, (xxxx), 1–8.
- [3] Chaplin J.R., Bearman P.W., Cheng Y., et al. Blind predictions of laboratory measurements of vortex-induced vibrations of a tension riser. *Journal of Fluids and Structures*, 2005a, 21(1 SPEC. ISS.), 25–40.
- [4] Chaplin J.R., Bearman P.W., Huera Huarte F.J., et al. Laboratory measurements of vortex-induced vibrations of a vertical tension riser in a stepped current[J]. *Journal of Fluids and Structures*, 2005b, 21(1 SPEC. ISS.), 3–24.
- [5] Chen W.M., Fu Y.Q., Guo S.X., et al. Fluid-solid coupling and hydrodynamic response of vortex-induced vibration of slender ocean cylinders[J]. *Advances in Mechanics*, 2016, 38(05):604.

- [6] Duan M.Y., Wan D.C., Xue H.X. Prediction of response for vortex-induced vibrations of a flexible riser pipe by using multi-strip method[C] Proceedings of the Twenty-sixth (2016) International Ocean and Polar Engineering Conference Rhodes, Greece, June 26-July 1, 2016, pp. 1065-1073.
- [7] Duan M.Y., Zou L., Wan D.C. Numerical analysis of multi-modal vibrations of a vertical riser in step currents[J]. *Ocean Engineering*, 2018, 152: 428-442.
- [8] Fu B.W., Duan M.Y., Wan D.C. Effect of mass ratio on the vortex-induced vibrations of a top tensioned riser[C]. Proceedings of the Second Conference of Global Chinese Scholars on Hydrodynamics, November 11-14, 2016, Wuxi, China, pp. 431-435.
- [9] Fu B.W., Zou L., Wan D.C. Numerical study of vortex-induced vibrations of a flexible cylinder in an oscillatory flow[J]. *Journal of Fluids and Structures*, 2018, 77:170-181.
- [10] Fu S.X., Wang J.G., Baarholm R., et al. VIV of Flexible Cylinder in Oscillatory Flow[C]. International Conference on Offshore Mechanics and Arctic Engineering, OMAE, June 9–14, 2013, Nantes, France, Volume 7: CFD and VIV ():V007T08A021.
- [11] Holmes S., Oakley O.H., Constantinides Y. Simulation of Riser VIV Using Fully Three Dimensional CFD Simulations[J]. International Conference on Offshore Mechanics and Arctic Engineering, OMAE, June 4–9, 2006, Hamburg, Germany, OMAE2006-92124.
- [12] Huang K., Chen H., Chen C.R. Riser VIV Analysis by a CFD Approach[C]. Proceedings of the Seventeenth (2007) International Ocean and Polar Engineering Conference, Lisbon, Portugal, July 1-6, 2007, pp2722–2729.
- [13] Huang K. and Chen C.R. Time-Domain Simulation of Riser VIV in Sheared Current[C]. International Conference on Offshore Mechanics and Arctic Engineering, OMAE, June 10–15, 2007, San Diego, California, USA, OMAE2007-29363.
- [14] Huang X.D., Zhang H., Wang X.S. An overview on the study of vortex-induced vibration of marine riser[J]. *Journal of Marine Sciences*, 2009, 27(04):95-101.
- [15] Lehn E. VIV Suppression Tests on High L/D Flexible Cylinders. 2003, Norwegian Marine Technology Research Institute, Trondheim, Norway.
- [16] Sarpkaya T. A critical review of the intrinsic nature of VIV[J]. *Fluid Mechanics and Its Applications*, 2004, 75:159–161.
- [17] Meneghini J.R., Saltara F., Fregonesi R.D.A., et al. Numerical simulations of VIV on long flexible cylinders immersed in complex flow fields[J]. *European Journal of Mechanics / B Fluids*, 2004, 23(1):51-63.
- [18] Wan D.C., Duan M.Y. A Recent Review of Numerical Studies on Vortex-Induced Vibrations of Long Slender Flexible Risers in Deep Sea[J]. *Chinese Quarterly of Mechanics*, 2017, 38(02):179-196.
- [19] Wang E. and Xiao, Q. Numerical simulation of vortex-induced vibration of a vertical riser in uniform and linearly sheared currents[J]. *Ocean Engineering*, 2016, 121, 492–515.
- [20] Willden R.H.J., Graham J.M.R. Numerical prediction of VIV on long flexible circular cylinders[J]. *Journal of Fluids & Structures*, 2001, 15(3-4):659-669.
- [21] Willden R.H.J., Graham J.M.R. Multi-modal Vortex-Induced Vibrations of a vertical riser pipe subject to a uniform current profile[J]. *European Journal of Mechanics, B/Fluids*, 2004, 23(1):209–218.
- [22] Yamamoto C.T., Meneghini J.R., Saltara F., et al. Numerical simulations of vortex-induced vibration on flexible cylinders[J]. *Journal of Fluids & Structures*, 2004, 19(4):467-489.